Separating direct and indirect effects of rising temperatures on biogenic volatile emissions in the Arctic

Riikka Rinnan[a,b,1], Lars L. Iversen[b,c], Jing Tang[a,b,d], Ida Vedel-Petersen[a], Michelle Schollert[a,b,e], and Guy Schurgers[b,f]

[a]Terrestrial Ecology Section, Department of Biology, University of Copenhagen, DK-2100 Copenhagen Ø, Denmark; [b]Center for Permafrost (CENPERM), University of Copenhagen, DK-1350 Copenhagen K, Denmark; [c]Department of Environmental Science, Policy, and Management, University of California, Berkeley, CA 94720; [d]Department of Physical Geography and Ecosystem Science, Lund University, SE-22362 Lund, Sweden; [e]Systems Ecology Section, Department of Ecological Science, Vrije Universiteit Amsterdam, 1081 HV Amsterdam, The Netherlands; and [f]Department of Geosciences and Natural Resource Management, University of Copenhagen, DK-1350 Copenhagen K, Denmark

Edited by Steven C. Wofsy, Harvard University, Cambridge, MA, and approved October 26, 2020 (received for review May 5, 2020)

Volatile organic compounds (VOCs) are released from biogenic sources in a temperature-dependent manner. Consequently, Arctic ecosystems are expected to greatly increase their VOC emissions with ongoing climate warming, which is proceeding at twice the rate of global temperature rise. Here, we show that ongoing warming has strong, increasing effects on Arctic VOC emissions. Using a combination of statistical modeling on data from several warming experiments in the Arctic tundra and dynamic ecosystem modeling, we separate the impacts of temperature and soil moisture into direct effects and indirect effects through vegetation composition and biomass alterations. The indirect effects of warming on VOC emissions were significant but smaller than the direct effects, during the 14-y model simulation period. Furthermore, vegetation changes also cause shifts in the chemical speciation of emissions. Both direct and indirect effects result in large geographic differences in VOC emission responses in the warming Arctic, depending on the local vegetation cover and the climate dynamics. Our results outline complex links between local climate, vegetation, and ecosystem–atmosphere interactions, with likely local-to-regional impacts on the atmospheric composition.

ecosystem–atmosphere interactions | climate change | vegetation change | ecosystem modelling

Biogenic VOCs, which are climate-relevant, short-lived gases, are produced and emitted from plant leaves following an exponential temperature dependency (1). Temperature increase accelerates the biosynthesis of VOCs and their diffusion from plant tissues. The Arctic is warming at an unprecedented pace (2), and, thus, we expect large increases in VOC emissions from tundra ecosystems. Indeed, experimental studies have shown that VOC emissions from tundra ecosystems in the Sub-Arctic (3, 4) and the Arctic (5–7) drastically increase under moderate warming. Known direct drivers of VOC emissions include temperature and photosynthetically active radiation (PAR), while indirect drivers could affect VOC emissions via changes in plant phenology or vegetation changes. However, we lack understanding of the overall relative importance of these direct and indirect drivers in the changing Arctic.

Arctic field experiments that use open-top chambers (OTCs) to raise the daytime air temperature by 1–4 °C during the growing season have shown that this warming causes severalfold increases in VOC emissions from ecosystem plots in dry (5, 7), mesic (4), and wet (6) tundra ecosystems. Further, the fast response to temperature changes in these experiments also suggests the emission increase to be a direct temperature effect on plant physiological processes; short-term warming experiments, which have been too short-lasting to cause any vegetation shifts, cause similar responses to long-term experiments (7). However, a field experiment that has run over a decade has shown that alterations in vegetation cover also influence the emissions (4). Weather conditions, especially temperature, of the previous weeks have been suggested to affect emission rates (8, 9). In the short growing season of the Arctic, this might be of special importance.

The Arctic climate has already warmed over recent decades—in some regions by as much as 1 °C per decade (10)—with documented effects on vegetation, including increases in shrub abundance and height (11). These vegetation changes may further promote warming via a vegetation-albedo feedback (12). The contribution of short-lived biogenic climate forcers, such as VOCs, to this warming has been poorly quantified. In the presence of nitrogen oxides (NO_X)—typically from anthropogenic sources—VOCs contribute to the formation of tropospheric ozone (13), which deteriorates the local air quality. However, in less polluted environments, the predominant atmospheric VOC sink is oxidation by hydroxyl radicals, a reaction which competes with methane oxidation (14). VOCs participate in secondary organic aerosol (SOA) formation and growth, which also takes place in environments with low background concentrations of anthropogenic pollution (15, 16). VOC-derived SOA has been

Significance

Plants release to the atmosphere reactive gases, so-called volatile organic compounds (VOCs). The release of VOCs from vegetation is temperature-dependent and controlled by vegetation composition because different plant species release a distinct blend of VOCs. We used modelling approaches on ecosystem VOC release data collected across the Arctic, which is experiencing both rapid warming and vegetation changes. We show that warming strongly stimulates release of plant-derived VOCs and that vegetation changes also increase VOC release, albeit less than temperature directly, and with large geographic differences in the Pan-Arctic area. The increasing VOC flux from the Arctic tundra to the atmosphere may have implications via climate feedbacks, for example, through particle and cloud formation in these regions with low anthropogenic influence.

Author contributions: R.R., L.L.I., J.T., I.V.-P., and G.S. designed research; R.R., I.V.-P., and M.S. performed research; L.L.I. and J.T. analyzed data; and R.R., L.L.I., and J.T. wrote the paper.

The authors declare no competing interest.

This article is a PNAS Direct Submission.

[1]To whom correspondence may be addressed. Email: riikkar@bio.ku.dk.

This article contains supporting information online at https://www.pnas.org/lookup/suppl/doi:10.1073/pnas.2008901117/-/DCSupplemental.

First published November 30, 2020.

suggested to reduce radiative forcing (i.e., cool the climate) both directly, owing to the light scattering impacts of SOA, as well as through its influence on cloud radiative properties (17). Feedbacks between biogenic processes resulting in SOA and cloud formation, as well as other SOA–cloud interactions, are nonlinear and poorly represented in models (18).

The atmospheric impacts of VOC emissions are not only dependent on the amount emitted but also on the composition of the emissions. Each plant species constitutively releases a distinct mixture of volatiles, and, as such, changes in vegetation composition have strong impacts on the quantity and composition of ecosystem emissions (19). Ongoing warming is shaping the tundra vegetation through a general "greening" tendency (11) and also by increasing the growth of deciduous shrubs in some areas (20) and evergreen shrubs in others (21). Such alterations to the vegetation composition have numerous impacts on ecosystems and climate feedbacks (21), including the amount and composition of locally emitted VOCs. To predict how climate change and the concomitant vegetation changes alter the tundra VOC emissions, we need to be able to separate the direct and indirect drivers of emissions.

Here, we explore relationships between VOC drivers and emissions using statistical modeling. We also use a dynamic vegetation model to quantify the importance of the direct effects of warming and indirect effects, via vegetation changes, on VOC emissions. In this cross-site analysis, we assess the patterns in ecosystem-scale VOC emissions as affected by the current or preceding temperature, PAR, soil moisture, and plant species composition. We first analyze plot-scale data collected in climate warming experiments in Northern Sweden and several Greenlandic locations, ranging from the Sub-Arctic to the High Arctic, during several years (see Dataset S1 for information about the sites). The low-statured vegetation in tundra ecosystems allows for measurements of VOCs at the ecosystem scale after experimental manipulation to study the effects of warming in replicated experimental designs. Data are first subjected to a multivariate statistical model to estimate the effect size on tundra VOC emission of daily temperatures, soil moisture, and PAR, as well as lagged effects of temperature within a season. Then, we use structural equation modeling (SEM) to compare the importance of the direct effects of temperature on VOC emissions with the indirect effects mediated by vegetation composition changes and to contrast effects of temperature and soil moisture. Finally, we assess Pan-Arctic VOC emissions using the dynamic vegetation model, LPJ-GUESS (22), to compare the effects of rising temperature alone with the combined effects of rising temperature and the warming-induced vegetation changes.

Results and Discussion

Biogenic VOCs comprise thousands of different chemical species. Here, we grouped the compounds into monoterpenes (MT; C_{10} terpenoids, typical plant volatiles that can be released both from de novo synthesis and from storage pools), sesquiterpenes (SQT; C_{15} terpenoids, plant volatiles, also known to be released from soil fungi, ref. 23), oxygenated monoterpenes (oMT), other reactive volatile organic compounds (ORVOCs, nonterpenoid compounds with atmospheric lifetime <24 h), and other volatile organic compounds (OVOCs, other nonterpenoids). Isoprene, which is the single most emitted biogenic VOC globally, was analyzed independently.

We used statistical modeling to estimate the effects of PAR, soil moisture, and temperature during VOC sampling, as well as the effects of the mean temperature of the preceding month (30-d period prior to the given day) and the 30- to 60-d period prior to the given day. The chamber temperature during sampling had the strongest positive impact on the emission of all terpenoids, followed by ORVOCs (first image in Fig. 1 and *SI Appendix*, Fig. S1). Except for isoprene and ORVOC emissions, which were not affected by the mean temperature of the preceding month, terpenoids and OVOCs were positively affected by the lagged temperature effect (second image in Fig. 1). This difference is likely due to contrasting biochemistry: While isoprene is emitted without storage upon de novo synthesis, other terpenoids can be produced over longer periods and evaporated from storage pools at a later date in a temperature-dependent manner (24). This is further confirmed by the strong, positive impact of PAR on the light-dependent emissions of isoprene, and lack of PAR effects on the other VOCs (fourth image in Fig. 1). Isoprene emission has been shown to depend on temperatures over the past days in earlier leaf level studies, and this effect is included in the commonly used VOC emission model, MEGAN, with the past 24- and 240-h air temperatures affecting emissions (9). The mean temperature of the 30–60 d preceding sampling that were tested in our study had a strong positive relationship with SQT emissions

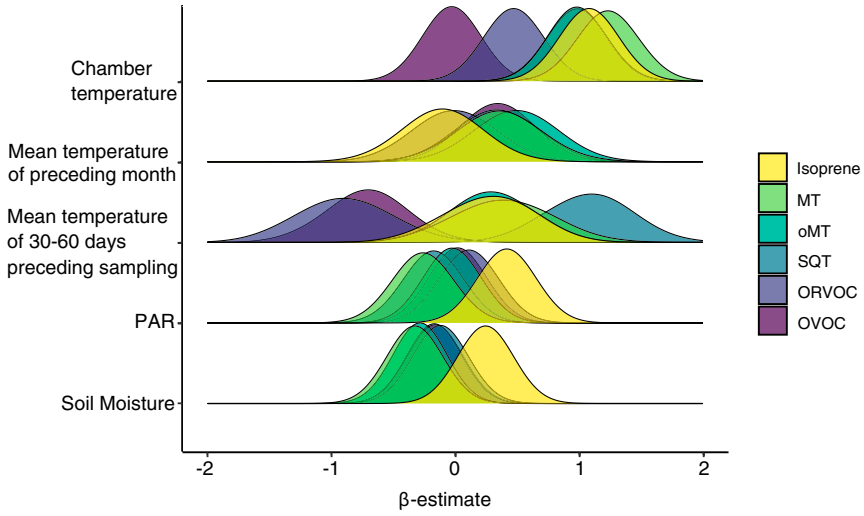

Fig. 1. Effects of environmental variables on VOC emissions. Density distributions of mean standardized effect sizes of five environmental variables in six different VOC groups. The effect sizes (β-estimates) correspond to linear slope parameters derived from multivariable mixed effect models containing sampling year, study site, and local habitat manipulation as random effects (see *SI Appendix*, Table S1 and Fig. S1 for further details). All β-estimates are adjusted for seasonal variation in VOC emissions, assuming an increase in the spring and a decrease in late summer.

and negative relationships with ORVOC and OVOC emissions (third image in Fig. 1). In the short Arctic growing season, these relationships highlight the importance of vegetation phenology and different ecosystem processes in controlling emissions in the different parts of the short Arctic growing seasons: SQTs, which are emitted by vegetation (25), soil (26), and litter decomposition (27, 28), have higher emissions if the spring or early growing season has been warm. In contrast, the relative importance of ORVOCs and OVOCs, which include compounds that are characteristic in soil emissions (29), decreases with a warmer early season.

The effect of temperature was most specific for the actual temperature (the temperature in the measurement chamber) and the predictive uncertainty (the width of the curves in Fig. 1) increased for the mean temperature of the 30- and 60-d periods preceding the measurement.

Soil moisture tended to have a negative relationship with MT and oMT emissions and a positive relationship with isoprene emissions (fifth image in Fig. 1). This is likely an indirect effect resulting from soil moisture control on vegetation composition or vegetation response to moisture conditions, the impacts of which were further assessed by SEM.

For each VOC group, we created a SEM to compare the direct effects of the chamber temperature (~ canopy air temperature) and soil moisture to indirect effects driven by vegetation community differences independent of the seasonal changes (Fig. 2*A*). The SEMs were constructed based on July measurements, which represent the peak growing season, and potential seasonality-related feedbacks were thus excluded. The plant species composition data were condensed into four principal components (PCs), which were used to describe the vegetation community (*SI Appendix*, Fig. S2). PAR was included in all models.

All SEM models provided a close fit between model and data (*SI Appendix*, Table S2; see Dataset S3 for summary statistics and parameter estimates). Vegetation composition affected the emissions of all VOC groups (*SI Appendix*, Fig. S3), except OVOCs, for which there were no significant effects of any parameter in the data used. In general, emissions of all other VOC groups were largely controlled by strong direct effects of temperature and indirect effects mediated by soil moisture shaping the vegetation community (Fig. 2*C*). Emissions of isoprene (Fig. 2*B*) and oMTs (*SI Appendix*, Fig. S3) were directly affected by both PAR and temperature. Emissions of MTs, SQTs, and ORVOCs were directly affected by temperature, but not PAR (*SI Appendix*, Fig. S3). Soil moisture had a direct negative impact on the emissions of ORVOCs, while having a positive indirect vegetation-mediated impact on the other VOC groups. For example, soil moisture had an indirect impact on isoprene emission, via correlation with the presence of the PC2-type vegetation, with main contributions by graminoids, lichens, the evergreen shrubs *Cassiope tetragona* and *Empetrum hermaphroditum*, willows (*Salix* spp.), and mosses (Fig. 2*B* and *SI Appendix*, Fig. S2).

In order to assess the relative importance of temperature increases and vegetation changes at larger scales, we used the process-based, dynamic ecosystem model, LPJ-GUESS (Lund-Potsdam-Jena-General Ecosystem Simulator, ref. 22). LPJ-GUESS links the synthesis of plant VOCs to photosynthesis, by assigning a fraction of the electron flux generated for photosynthesis to terpenoid synthesis (30, 31). The model currently includes processes for modeling isoprene and MT emissions, and Tang et al. (32) adjusted the model for tundra VOC emissions based on leaf-level emission factors measured in situ and included a stronger temperature response, as has been observed for tundra ecosystems. Since the model mechanistically represents plant establishment, mortality, disturbance, and growth, as well as soil biogeochemical processes in response to input climate variability, it enables us to separate the direct effects of warming from the indirect, vegetation change-related effects.

We compared two different scenarios: one in which warming only affects the VOC production rate and emission, but without warming-induced vegetation changes (direct effects, DIR), and one in which warming affects both the VOC production and emission, as well as vegetation dynamics (direct + indirect effects, DIR+IND). Both effects were simulated with a 2 °C or 4 °C temperature increase for the time period of 1999–2012 in the entire study area, resulting in four designed scenario simulations. These simulations were compared with the control simulation with current climate. The simulated vegetation distribution in the control simulation (*SI Appendix*, Fig. S4) was largely in agreement with the Circumpolar Arctic Vegetation Map (33), International Geosphere–Biosphere Programme Land Cover (34), and with Kaplan et al. (35), with some regional differences between the modeled distribution and these published maps (such as the potential overestimation of needle-leaved summergreen tree presence along the northern coast of Russia). The results below compare the emission differences caused by direct (DIR) and indirect effects (IND) of warming, where the direct effects were quantified as the difference between the scenario run of DIR and the control run, and the indirect effects were quantified as the difference between the scenarios run of DIR+IND and the scenarios run of DIR.

Warming alone caused large increases in annual isoprene and MT emissions averaged across the Pan-Arctic region, with larger increases for 4 °C than 2 °C warming (Fig. 3). Including indirect temperature effects (e.g., via phenology, vegetation dynamics, and plant physiological processes under a warmer climate allowing for longer growing seasons) further enhanced this increase, but with relatively smaller magnitude compared to the direct warming effects. For isoprene, the indirect temperature effects in this region become more and more important over time, linking to the gradually increasing vegetation coverage and/or the increasing relative contributions of isoprene-emitting species to the total vegetation cover (i.e., shade-intolerant broadleaved summergreen trees [IBS] and temperate shade-tolerant broadleaved summergreen trees [TeBS]). For monoterpenes, the impact of indirect effects was considerably smaller than for isoprene, and more constant over time. The apparent peak in the MT response to the indirect effects of warming in 1999 (Fig. 3*B*), compared to other years, is due to a larger relative effect of the temperature increase on the length of the growing season and the positive consequences of this on the plant growth of MT emitters. While the chemical speciation of the emissions, assessed here as the ratio between isoprene and MT emissions, was largely unaffected by the direct effects of warming, it changed rapidly and strongly in response to the indirect effects of warming (Fig. 3*C*). We estimate that VOC emissions from the Pan-Arctic become even more strongly dominated by isoprene than presently, as a result of vegetation shifts caused by warming.

Warming alone increased isoprene production and emission over the ice-free Pan-Arctic, when averaged across the period 1999–2012, with the largest relative increases in the High and Low Arctic areas of North America and several regions in Siberia (Fig. 4 *A* and *C*). Warming-induced vegetation changes caused both decreases and increases in isoprene emissions depending on the location (Fig. 4 *B* and *D*). Overall, we observed similar patterns for MTs (*SI Appendix*, Fig. S5). In general, the increase in isoprene emissions was most pronounced in the High Arctic, where isoprene-emitting grasses and mosses (36–38), as well as shrubs (39, 40), increase in abundance (*SI Appendix*, Fig. S6). Isoprene emissions decreased with the warming-induced vegetation changes in the southernmost areas of the current Subarctic North America and Western Russia (Fig. 4), due to a slight decrease in tree coverage (*SI Appendix*, Fig. S6). This decrease may be related to reduced plant productivity, due to

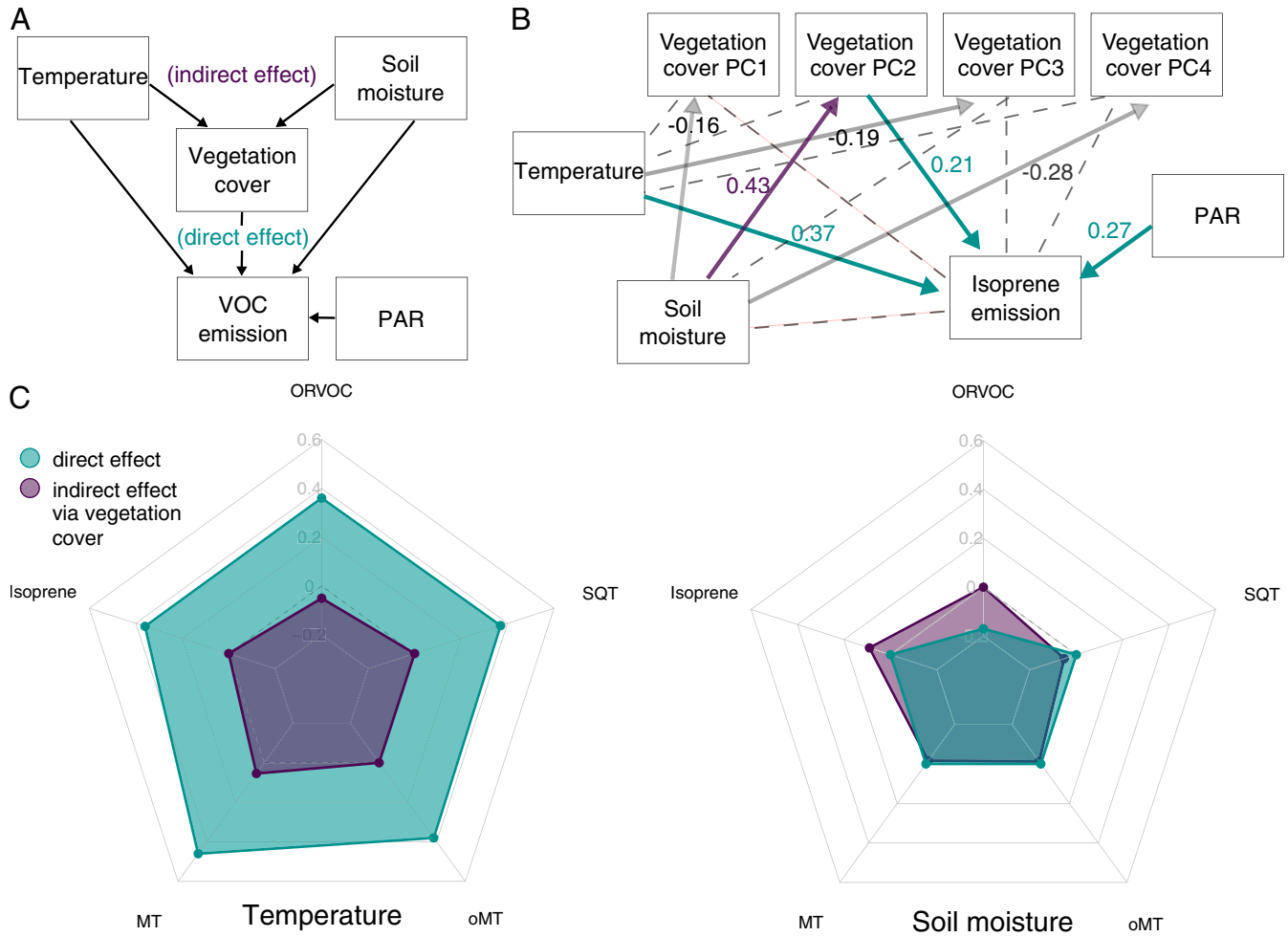

Fig. 2. Structural equation models representing direct and indirect linkages of environmental factors on VOC emission. (*A*) The conceptual model tested, in which temperature and soil moisture affect VOC emissions directly or indirectly by structuring the vegetation cover. (*B*) An example of a final SEM model for isoprene emission. Solid arrows represent significant linear paths supported by the model; dashed lines are omitted paths. Values represent standardized effect sizes. (*C*) Effect sizes on each VOC group summed across the SEM models for temperature and soil moisture, respectively. Direct effect sizes (green) correspond to parameter estimates between VOC and the given parameter. Indirect effects (purple) correspond to the mediated effect of a variable via the vegetation cover PC axis. All numbers are scaled to z-scores in order to enable comparisons of effect sizes across variable types. All deviations from 0 are significant.

summer drought, resulting from increased evapotranspiration with higher temperatures and earlier onset of the growing season in the southern forest areas (41).

We found that the highest relative increases in isoprene and MT emissions, both due to warming and vegetation changes, are likely to occur in the High Arctic (Fig. 4 and *SI Appendix*, Fig. S5). *SI Appendix*, Figs. S7 and S8 show the absolute changes in isoprene and MT emissions. The large increase in VOC emissions in the High Arctic is associated with shrub expansion and biomass growth (42) in this region (*SI Appendix*, Fig. S6). The decrease in MT emissions caused by warming-induced vegetation changes occurs widely in boreal forest due to replacement of moderate MT-emitter plant functional types (PFTs) (boreal needle-leaved evergreen trees) with low MT-emitter PFTs (temperate broad-leaved summergreen trees) in response to the temperature increase.

Recent climate modeling studies suggest that considering a scenario with a 2 °C or 4 °C temperature increase for the Arctic might not be unrealistic in a long term. In fact, a 2 °C increase in mean annual temperature in the Arctic (relative to 1981–2005 baseline mean) is expected in 25 y under the Representative Concentration Pathway (RCP) 8.5 of the Intergovernmental Panel on Climate Change (the so-called "business as usual" scenario) and in 50 y with RCP 4.5 (moderate mitigation scenario, ref. 43). Arctic warming is expected to be most pronounced in the late boreal autumn, when temperature increases may be as high as 13 °C by the end of this century (following RCP 8.5, ref. 43). Warming is highly relevant for tundra VOC emissions, which increase steeply with temperature above a minimum temperature of ∼10 °C (32, 44). Furthermore, prolongation of the growing season due to warming not only extends the period of potentially high biological activity, but also leads to alterations in phenology and vegetation composition (42, 45), which were accounted for in our simulations considering the indirect effects of warming.

In summary, we show that ongoing warming has strong direct increasing effects on VOC emissions from Arctic ecosystems and also indirect effects resulting from prolongation of the growing season length and alterations in vegetation composition and biomass. Shifts in the chemical speciation of the emissions are accompanied with large geographic differences. Changes in VOC emissions are likely to have local-to-regional impacts on

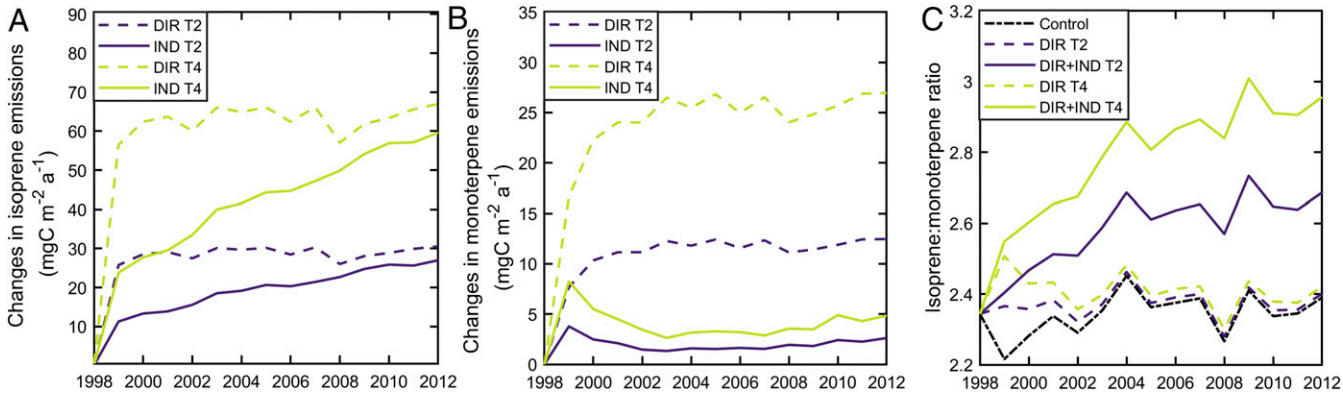

Fig. 3. Changes in modeled annual isoprene (*A*) and monoterpene (*B*) emissions due to direct and indirect effects, and the isoprene-to-monoterpene ratio for emissions (*C*) from each model simulation averaged over the Pan-Arctic land area. DIR were determined from the difference between the scenarios with 2 °C (DIR T2) or 4 °C (DIR T4) warming impacts on VOC production/emission and the control run. IND were determined from the difference between the simulations with both direct and indirect effects and those with only direct effects. Note the different *y* axis scales.

atmospheric composition, via oxidation reactions and particle formation.

Materials and Methods

Datasets and Locations. We used data collected from climate warming experiments in European Subarctic and Arctic locations during 2006–2015. The locations were Abisko in Northern Sweden (68°21′ N, 18°49′ E, Subarctic), Disko Island (69°14′ N, 53°32′ W) and Kobbefjord (64°7′ N, 51°21′ W) in Western Greenland (Low Arctic), and Zackenberg in Northeastern Greenland (74°30′ N, 20°30′ W, High Arctic). Data from the mesic heath in Abisko have been previously published (3, 4, 46). Data from Disko Island includes results from a dry low shrub tundra (7) and a graminoid-dominated wetland (6). Those from Kobbefjord were collected on a dry tundra dominated by *Salix glauca* and *E. hermaphroditum* (5). Data from Zackenberg include measurements in four contrasting vegetation types (47), across a soil moisture gradient (48) and previously unpublished data from a climate warming experiment. Climatic information, emission data, and environmental conditions during the measurements for each location are summarized in Dataset S1.

VOC Emission Measurements. VOC emissions were measured from 22 × 22 cm plots of tundra (except for Kobberfjord, where the plot size was 33 × 33 cm) consisting of an intact vegetation cover of the site and the soil beneath. The plots were bordered by aluminum frames that extended to ca. 10 cm depth in soil and provided a base for the flux measurement chamber. These frames had been installed in the plots a minimum of 1 y before starting the measurements. During measurements, conducted by the push–pull enclosure technique, a transparent polycarbonate chamber was placed on the aluminum base. The chamber headspace (volumes typically approx. 9.6 L, in Kobberfjord 25 L) was mixed with a fan, and air was circulated through via

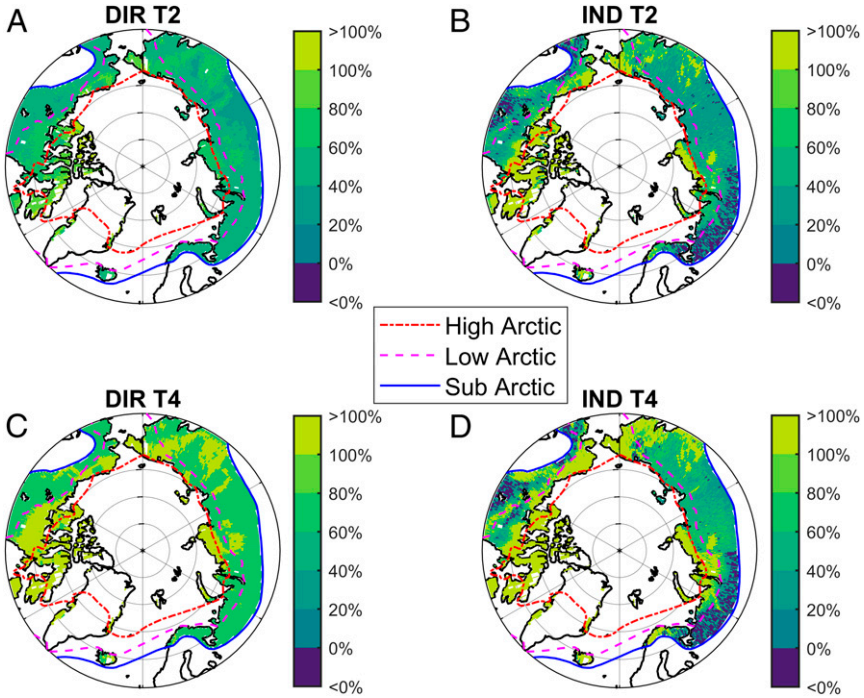

Fig. 4. Relative changes in isoprene emission under direct and indirect effects of warming by 2 °C (*A* and *B*) and 4 °C (*C* and *D*). *A* and *C* show the DIR on isoprene production and emission rate, and (*B* and *D*) show the IND mainly through changes in vegetation composition and vegetation-related processes averaged for the period 1999–2012.

battery-operated pumps, with a flow rate of 200 mL·min^{-1} (in some cases, inflow was maintained at 215 mL·min^{-1}). The replacement air was purified by a charcoal filter to remove particles and VOCs present in ambient air and by a manganese oxide scrubber or copper tubing coated with potassium iodide to remove ozone (49). The sampled air was pulled through stainless steel adsorbent cartridges packed with 150 mg of Tenax TA and 200 mg of Carbograph 1 TD. VOCs were analyzed after thermal desorption (Unity 2 thermal desorber coupled with an Ultra autosampler; Markes International Limited) on a gas chromatograph-mass spectrometer (7890A Series GC, 5975C inert MSD/DS Performance Turbo EI, Agilent Technologies).

At each site, blank samples were collected by placing a polyethylene terephthalate sheet in between the measurement chamber and the ecosystem, and then sampling VOCs as for actual samples. The VOC concentrations in the blanks were subtracted from the samples, and in some cases the major compounds in blanks were considered impurities and completely removed from the data. All other compounds—whether available as calibration standards or only tentatively identified by the National Institute of Standards and Technology mass spectral library—were included in the data. Details on the measurement and analytical methods, quantification, and compound identification are provided in the original publications.

The individual compounds were grouped into the following classes (50): isoprene, monoterpenes (includes monoterpenoids), oxygenated monoterpenes, sesquiterpenes (includes sesquiterpenoids), ORVOCs (lifetime less than 1 d), and OVOCs.

Vegetation Analysis. The cover percentage of each plant species in the plots was estimated using the point intercept method (51). A pin was vertically lowered in each grid point, and a hit was recorded every time the pin touched a vascular plant, moss, lichen, litter, or soil. This analysis gives a three-dimensional picture of the vegetation cover, and the cover may exceed 100%.

Monitoring of Environmental Conditions. Air temperature and relative humidity inside the VOC measurement chamber were recorded (Hygrochron DS 1923-F5 iButton, Maxim Integrated Products Inc.) once a minute during VOC sampling. PAR was recorded every 10 s using PAR sensors (S-LIA-M003, Onset Computer Corporation) coupled to a Hobo Micro Station data logger. Values were averaged for the VOC sampling period (typically 30 min). Soil moisture was measured manually in topsoil (ML3 Theta Probe Soil Moisture Sensor, Delta-T Devices). In addition, data for ambient air temperature were collected from climate station databases administered by Greenland Ecosystem Monitoring and Abisko Scientific Research Station. Ambient air temperature was a diel average of temperature measured at 2–3 m height close to VOC measurement sites.

Statistical Modeling. Multivariate linear mixed effect models were used to estimate effect of temperature and other environmental variables on VOC emissions. For each individual VOC class, we created a presence only model, estimating effect sizes of environmental variables during VOC emission measurements. For each VOC class, we constructed a model including the fixed effects of daily PAR, daily measures of soil moisture, chamber temperatures during the VOC measurement, mean temperature 30 d prior to the given day, mean temperature 30–60 d prior to the given day, day of year, and day of year squared. Day of year was treated as a cofounding variable and modeled as a second-order polynomial, adjusting for any hump-shaped patterns in emission rates across season. We achieved general parameter estimates by adding random intercepts for individual measurement year, treatment (control or OTC warming), and study site. In order to ensure model conversion and enable model inference across random effects (52), all of the mixed models were fitted as Gaussian linear models and VOC emission data were log-transformed prior to any model run. All fixed environmental explanatory variables were standardized to a mean of zero and SD of one. This allowed for the comparison of effect sizes (the slope-β estimates in models) across the explanatory variables. Estimated uncertainties for each β are shown in *SI Appendix*, Table S1. The level of variance explained by each component model for all response variables is given as the conditional R^2 (or pseudo R^2) based on the variance of both the fixed and random effects (53).

Structural Equation Modeling. We used SEM to evaluate the direct effects of temperature and soil moisture, as well as indirect effects via vegetation cover, on VOC emissions during peak growing season (only July data included). In SEM, causal links between variables of interest are defined and evaluated in the form of interconnected equations (54, 55).

We created a conceptual model with a hypothetical path diagram in which plot-level temperature and soil moisture had an indirect effect on VOC emissions by affecting vegetation cover. Plot-level vegetation covers were condensed into four PC axes explaining 67.4% of the variation in the species composition data by principal component analysis (PCA; *SI Appendix*, Fig. S2). The PCA was based on log(cover +1) of all of the plant data merged into 16 groups representing correlated unities (56).

In the SEM, all endogenous variables were modeled using linear Gaussian mixed effect models, containing measurement year, treatment (control or OTC warming), and study site as random intercepts, and the explanatory variables as fixed effects. Furthermore, we adjusted the models for daily variation in radiation levels by adding PAR as a covariate. Each model was screened for residual distributional properties. In order to meet the assumption of variable homogeneity, we log-transformed the single VOC measures prior to analysis.

We evaluated the full SEM and potential inclusion of missing paths using Fisher's C statistic (57). In contrast to globally estimated models, local estimators permit complex path specifications fitted by the entire covariance matrix and do not transfer misspecification errors across different parts of an SEM (58). In each of the local models, the links supported by our data were identified via a two-way ANOVA test (59). For each VOC group, we estimated conditional R^2 for the model component estimating direct effects.

In order to contrast the importance between the different model components, effect sizes across the SEM were derived from path coefficients scaled to a mean of zero and SD of one. The direct effect size of temperature and soil moisture, and indirect effect sizes via vegetation cover, were established from the estimated parameters in the final SEMs. The indirect pathways via vegetation cover were defined as the sum across all four PCs of the product of temperature/soil moisture to vegetation cover and vegetation cover to VOC emission path.

All statistical modeling and SEM analyses were conducted in R version 3.5.3 using the piecewiseSEM v.1 (59), lme4 (60), and FactoMineR (61) packages.

Dynamic Ecosystem Modeling. LPJ-GUESS is a climate-driven dynamic ecosystem model, which has been widely used at the plot, regional, and global scales (22, 62–64). The model is process-based with mechanistic representation of vegetation dynamics, including establishment, mortality, competition for light, water and nutrient resources, and disturbance (65), and soil biogeochemistry (66). Vegetation in the model is represented by PFTs, which are defined by the bioclimatic limits for their establishment and mortality, and their plant physiological and physiognomic features. LPJ-GUESS has been applied and evaluated in a number of studies exploring Arctic vegetation dynamics (e.g., refs. 12, 62, and 63). An adapted Farquhar photosynthesis model (67, 68) is used for simulating daily photosynthesis. Isoprene (30) and MT (31) are simulated in the model as a function of the photosynthetic electron flux that is allocated to synthesis of these compounds. Whereas isoprene is emitted directly upon synthesis, monoterpenes can be stored in storage organs for some PFTs, followed by a temperature-dependent emission (31). Simulation of emissions of other VOCs has not yet been implemented in LPJ-GUESS.

In this study, we used the extended arctic PFTs based on ref. 32, in which the existing arctic leaf-level emission measurements were used to update the emission factors with further parameter adjustments for a few PFTs in consideration of species distribution in the Pan-Arctic region (Dataset S2). The high temperature response reported in Tang et al. (32) with beta value of 0.23 has been used for arctic PFTs, while the global temperature response curve (with beta value of 0.10) has been used for PFTs not specific to the Arctic tundra (Dataset S2).

A control simulation was performed for the Arctic region (north of 60°N and within the Pan-Arctic boundaries defined by the Conservation of Arctic Flora and Fauna) at a spatial resolution of 0.5° for the period 1901–2012. The climate inputs (monthly mean temperature, precipitation, radiation, monthly mean of daily maximum and minimum temperatures, and number of wet days) were obtained from CRU TS 3.21 (69), and the annual mean atmospheric CO_2 concentration was obtained from ref. 70. All runs were initialized by 300-y spin-up by recycling detrended 1901–1930 climate forcing to equilibrate vegetation and soil carbon pools.

In addition to the control simulation, four simulations with warming scenarios were applied in which temperatures were increased by 2 °C or 4 °C for the period 1999–2012, mimicking the climate warming experiments in the data analysis. Two of these scenarios applied a temperature increase in the computation of terpenoid synthesis only, hence representing a direct impact on emissions (referred to as DIR); the other two scenarios applied the temperature increase to all ecosystem processes including terpenoid synthesis, hence representing both direct and indirect impacts on emissions

(referred to as DIR+IND). Drivers other than temperature were the same as in the control simulation.

Data Availability. All data and R scripts used in this manuscript are publicly available and deposited in the Dryad Digital Repository (https://doi.org/10.5061/dryad.kh189323t) (71).

ACKNOWLEDGMENTS. The Abisko Scientific Research Station provided data of environmental variables from their weather station. Environmental data for Zackenberg, Disko, and Nuuk were provided by the Greenland Ecosystem Monitoring Programme. The field experiments were established and maintained by Anders Michelsen, Daan Blok, Niels Martin Schmidt, and Bo Elberling. Sarah Hagel Svendsen, Ingvild Ryde, and Tora Finnerup Nielsen assisted in field measurements in Zackenberg. We thank Cleo Davie-Martin for her comments. This work was financially supported by grants from the Villum Foundation, the Danish Council for Independent Research | Natural Sciences, the Carlsberg Foundation, the European Research Council under the European Union's Horizon 2020 research and innovation programme Grant 771012, and the Danish National Research Foundation (DNRF100 CENPERM) (to R.R.). J.T. was financially supported by European Union's Horizon 2020 research and innovation programme under Marie Sklodowska-Curie Grant 707187 and FORMAS mobility Grant 2016-01580). L.L.I. was funded by Carlsberg Foundation Grants CF17- 0155 and CF18-0062. The Pan-Arctic simulations described in this paper were performed using the Danish e-infrastructure Cooperation National Life Science Supercomputer at Technical University of Denmark.

1. A. B. Guenther, P. R. Zimmerman, P. C. Harley, R. K. Monson, R. Fall, Isoprene and monoterpene emission rate variability: Model evaluations and sensitivity analyses. *J. Geophys. Res. Atmos.* **98**, 12609–12617 (1993).
2. IPCC, *Climate Change 2013: The Physical Science Basis. Contribution of Working Group I to the Fifth Assessment Report of the Intergovernmental Panel on Climate Change*, T. F. Stocker, Ed. *et al*. (Cambridge University Press, Cambridge, United Kingdom, 2013).
3. P. Faubert *et al*., Doubled volatile organic compound emissions from subarctic tundra under simulated climate warming. *New Phytol.* **187**, 199–208 (2010).
4. H. Valolahti, M. Kivimäenpää, P. Faubert, A. Michelsen, R. Rinnan, Climate change-induced vegetation change as a driver of increased subarctic biogenic volatile organic compound emissions. *Glob. Change Biol.* **21**, 3478–3488 (2015).
5. M. Kramshøj *et al*., Large increases in Arctic biogenic volatile emissions are a direct effect of warming. *Nat. Geosci.* **9**, 349–352 (2016).
6. F. Lindwall, S. S. Svendsen, C. S. Nielsen, A. Michelsen, R. Rinnan, Warming increases isoprene emissions from an arctic fen. *Sci. Total Environ.* **553**, 297–304 (2016).
7. F. Lindwall, M. Schollert, A. Michelsen, D. Blok, R. Rinnan, Fourfold higher tundra volatile emissions due to arctic summer warming. *J. Geophys. Res. Biogeosci.* **121**, 895–902 (2016).
8. G. Pétron, P. Harley, J. Greenberg, A. Guenther, Seasonal temperature variations influence isoprene emission. *Geophys. Res. Lett.* **28**, 1707–1710 (2001).
9. A. Guenther *et al*., Estimates of global terrestrial isoprene emissions using MEGAN (model of emissions of gases and aerosols from nature). *Atmos. Chem. Phys.* **6**, 3181–3210 (2006).
10. J. Huang *et al*., Recently amplified arctic warming has contributed to a continual global warming trend. *Nat. Clim. Chang.* **7**, 875–879 (2017).
11. S. C. Elmendorf *et al*., Plot-scale evidence of tundra vegetation change and links to recent summer warming. *Nat. Clim. Chang.* **2**, 453–457 (2012).
12. P. A. Miller, B. Smith, Modelling tundra vegetation response to recent arctic warming. *Ambio* **41** (suppl. 3), 281–291 (2012).
13. R. Atkinson, Atmospheric chemistry of VOCs and NOx. *Atmos. Environ.* **34**, 2063–2101 (2000).
14. P. S. Monks *et al*., Tropospheric ozone and its precursors from the urban to the global scale from air quality to short-lived climate forcer. *Atmos. Chem. Phys.* **15**, 8889–8973 (2015).
15. F. Bianchi *et al*., New particle formation in the free troposphere: A question of chemistry and timing. *Science* **352**, 1109–1112 (2016).
16. J. Tröstl *et al*., The role of low-volatility organic compounds in initial particle growth in the atmosphere. *Nature* **533**, 527–531 (2016).
17. D. V. Spracklen, B. Bonn, K. S. Carslaw, Boreal forests, aerosols and the impacts on clouds and climate. *Philos. Trans.- Royal Soc., Math. Phys. Eng. Sci.* **366**, 4613–4626 (2008).
18. M. Shrivastava *et al*., Recent advances in understanding secondary organic aerosol: Implications for global climate forcing. *Rev. Geophys.* **55**, 509–559 (2017).
19. A. Arneth, U. Niinemets, Induced BVOCs: How to bug our models? *Trends Plant Sci.* **15**, 118–125 (2010).
20. I. H. Myers-Smith *et al*., Shrub expansion in tundra ecosystems: Dynamics, impacts and research priorities. *Environ. Res. Lett.* **6**, 045509 (2011).
21. T. Vowles, R. G. Björk, Implications of evergreen shrub expansion in the Arctic. *J. Ecol.* **107**, 650–655 (2019).
22. B. Smith *et al*., Implications of incorporating N cycling and N limitations on primary production in an individual-based dynamic vegetation model. *Biogeosciences* **11**, 2027–2054 (2014).
23. E. Horváth *et al*., Microscopic fungi as significant sesquiterpene emission sources. *J. Geophys. Res. Atmos.* **116**, D16301 (2011).
24. J. Laothawornkitkul, J. E. Taylor, N. D. Paul, C. N. Hewitt, Biogenic volatile organic compounds in the Earth system. *New Phytol.* **183**, 27–51 (2009).
25. T. R. Duhl, D. Helmig, A. Guenther, Sesquiterpene emissions from vegetation: A review. *Biogeosciences* **5**, 761–777 (2008).
26. E. Bourtsoukidis *et al*., Strong sesquiterpene emissions from Amazonian soils. *Nat. Commun.* **9**, 2226 (2018).
27. J. P. Greenberg *et al*., Contribution of leaf and needle litter to whole ecosystem BVOC fluxes. *Atmos. Environ.* **59**, 302–311 (2012).
28. S. H. Svendsen *et al*., Emissions of biogenic volatile organic compounds from arctic shrub litter are coupled with changes in the bacterial community composition. *Soil Biol. Biochem.* **120**, 80–90 (2018).
29. J. Tang, G. Schurgers, R. Rinnan, Process understanding of soil BVOC fluxes in natural ecosystems: A review. *Rev. Geophys.* **57**, 966–986 (2019).
30. A. Arneth *et al*., Process-based estimates of terrestrial ecosystem isoprene emissions: Incorporating the effects of a direct CO_2-isoprene interaction. *Atmos. Chem. Phys.* **7**, 31–53 (2007).
31. G. Schurgers, A. Arneth, R. Holzinger, A. H. Goldstein, Process-based modelling of biogenic monoterpene emissions combining production and release from storage. *Atmos. Chem. Phys.* **9**, 3409–3423 (2009).
32. J. Tang *et al*., Challenges in modelling isoprene and monoterpene emission dynamics of arctic plants: A case study from a subarctic tundra heath. *Biogeosciences* **13**, 6651–6667 (2016).
33. D. A. Walker *et al*., The circumpolar arctic vegetation map. *J. Veg. Sci.* **16**, 267–282 (2005).
34. M. A. Friedl *et al*., ISLSCP II MODIS (collection 4) IGBP land cover, 2000-2001 (2010). https://doi.org/10.3334/ORNLDAAC/968. Accessed 10 February 2020.
35. J. O. Kaplan *et al*., Climate change and Arctic ecosystems: 2. Modeling, paleodata-model comparisons, and future projections. *J. Geophys. Res. Atmos.* **108**, 8171 (2003).
36. A. Ekberg, A. Arneth, H. Hakola, S. Hayward, T. Holst, Isoprene emission from wetland sedges. *Biogeosciences* **6**, 601–613 (2009).
37. D. T. Hanson, S. Swanson, L. E. Graham, T. D. Sharkey, Evolutionary significance of isopreneemission from mosses. *Am. J. Bot.* **86**, 634–639 (1999).
38. A. Ekberg, A. Arneth, T. Holst, Isoprene emission from *Sphagnum* species occupying different growth positions above the water table. *Boreal Environ. Res.* **16**, 47–59 (2011).
39. M. J. Potosnak *et al*., Isoprene emissions from a tundra ecosystem. *Biogeosciences* **10**, 871–889 (2013).
40. I. Vedel-Petersen, M. Schollert, J. Nymand, R. Rinnan, Volatile organic compound emission profiles of four common arctic plants. *Atmos. Environ.* **120**, 117–126 (2015).
41. A. Bastos *et al*., Direct and seasonal legacy effects of the 2018 heat wave and drought on European ecosystem productivity. *Sci. Adv.* **6**, eaba2724 (2020).
42. T. Park *et al*., Changes in growing season duration and productivity of northern vegetation inferred from long-term remote sensing data. *Environ. Res. Lett.* **11**, 084001 (2016).
43. E. Post *et al*., The polar regions in a 2°C warmer world. *Sci. Adv.* **5**, eaaw9883 (2019).
44. Roger Seco *et al*., Volatile organic compound fluxes in a subarctic peatland and lake. *Atmos. Chem. Phys.* **20**, 13399–13416 (2020).
45. H. W. Linderholm, Growing season changes in the last century. *Agric. For. Meteorol.* **137**, 1–14 (2006).
46. P. Tiiva *et al*., Climatic warming increases isoprene emission from a subarctic heath. *New Phytol.* **180**, 853–863 (2008).
47. M. Schollert, S. Burchard, P. Faubert, A. Michelsen, R. Rinnan, Biogenic volatile organic compound emissions in four vegetation types in high arctic Greenland. *Polar Biol.* **37**, 237–249 (2014).
48. S. H. Svendsen, F. Lindwall, A. Michelsen, R. Rinnan, Biogenic volatile organic compound emissions along a high arctic soil moisture gradient. *Sci. Total Environ.* **573**, 131–138 (2016).
49. J. Ortega, D. Helmig, Approaches for quantifying reactive and low-volatility biogenic organic compound emissions by vegetation enclosure techniques - part A. *Chemosphere* **72**, 343–364 (2008).
50. A. Guenther *et al*., A global model of natural volatile organic compound emissions. *J. Geophys. Res. Atmos.* **100**, 8873–8892 (1995).
51. S. Jonasson, Evaluation of the point intercept method for the estimation of plant biomass. *Oikos* **52**, 101–106 (1988).
52. W. W. Stroup, *Generalized Linear Mixed Models: Modern Concepts, Methods and Applications* (CRC Press, 2016).
53. S. Nakagawa, H. Schielzeth, A general and simple method for obtaining R^2 from generalized linear mixed-effects models. *Methods Ecol. Evol.* **4**, 133–142 (2013).
54. B. Shipley, Confirmatory path analysis in a generalized multilevel context. *Ecology* **90**, 363–368 (2009).
55. J. B. Grace, *Structural Equation Modeling and Natural Systems* (Cambridge University Press, 2006).
56. P. Legendre, L. F. Legendre, *Numerical Ecology* (Elsevier, 2012), vol. 24.
57. B. Shipley, A new inferential test for path models based on directed acyclic graphs. *Struct. Equ. Modeling* **7**, 206–218 (2000).
58. K. A. Bollen, J. B. Kirby, P. J. Curran, P. M. Paxton, F. Chen, Latent variable models under misspecification: Two-stage least squares (2SLS) and maximum likelihood (ML) estimators. *Sociol. Methods Res.* **36**, 48–86 (2007).
59. J. S. Lefcheck, piecewiseSEM: Piecewise structural equation modelling in r for ecology, evolution, and systematics. *Methods Ecol. Evol.* **7**, 573–579 (2016).
60. D. Bates, M. Maechler, B. Bolker, S. Walker, {lme4}: Linear mixed-effects models using Eigen and S4. *R Package Version* **1**, 1–13 (2014).

61. S. Lê, J. Josse, F. Husson, FactoMineR: An R package for multivariate analysis. *J. Stat. Softw.* **25**, 1–18 (2008).
62. A. Wolf, T. V. Callaghan, K. Larson, Future changes in vegetation and ecosystem function of the Barents region. *Clim. Change* **87**, 51–73 (2008).
63. J. Tang *et al*., Carbon budget estimation of a subarctic catchment using a dynamic ecosystem model at high spatial resolution. *Biogeosciences* **12**, 2791–2808 (2015).
64. T. Hickler *et al*., Projecting the future distribution of European potential natural vegetation zones with a generalized, tree species-based dynamic vegetation model. *Glob. Ecol. Biogeogr.* **21**, 50–63 (2012).
65. B. Smith, I. C. Prentice, M. T. Sykes, Representation of vegetation dynamics in the modelling of terrestrial ecosystems: Comparing two contrasting approaches within European climate space. *Glob. Ecol. Biogeogr.* **10**, 621–637 (2001).
66. S. Sitch *et al*., Evaluation of ecosystem dynamics, plant geography and terrestrial carbon cycling in the LPJ dynamic global vegetation model. *Glob. Change Biol.* **9**, 161–185 (2003).
67. G. J. Collatz, J. T. Ball, C. Grivet, J. A. Berry, Physiological and environmental regulation of stomatal conductance, photosynthesis and transpiration: A model that includes a laminar boundary layer. *Agric. For. Meteorol.* **54**, 107–136 (1991).
68. G. D. Farquhar, S. von Caemmerer, J. A. Berry, A biochemical model of photosynthetic CO_2 assimilation in leaves of C 3 species. *Planta* **149**, 78–90 (1980).
69. P. D. Jones, I. C. Harris, *University of East Anglia Climatic Research Unit, CRU TS3. 21: Climatic Research Unit (CRU) Time-Series (TS) Version 3.21 of High Resolution Gridded Data of Month-by-Month Variation in Climate (Jan. 1901—Dec. 2012)* (NCAS British Atmospheric Data Centre, Leeds, United Kingdom, 2013).
70. Karl E. Taylor, Ronald J. Stouffer, Gerald A. Meehl, An overview of CMIP5 and the experiment design. *Bull. Am. Meteorol. Soc.* **93**, 485–498 (2012).
71. R. Rinnan *et al*., Data for: Separating direct and indirect effects of rising temperatures on biogenic volatile emissions in the Arctic. *Dryad*. https://doi.org/10.5061/dryad.kh189323t. Deposited 12 November 2020.